
Article:
Galvin, T., Hyatt, N.C., Rainforth, W.M. et al. (2 more authors) (2019) Laser sintering of electrophoretically deposited (EPD) Ti3SiC2 MAX phase coatings on titanium. Surface and Coatings Technology, 366. pp. 199-203. ISSN 0257-8972

https://doi.org/10.1016/j.surfcoat.2019.03.031

Laser sintering of electrophoretically deposited (EPD) Ti_3SiC_2 MAX phase coatings on titanium

T. Galvin[1*], N. C. Hyatt[1], W. M. Rainforth[1], I. M. Reaney[1], D. Shepherd[2]

1. Department of Materials Science and Engineering, University of Sheffield, Sir Robert Hadfield Building, Mappin St, Sheffield, S1 3JD, UK

2. National Nuclear Laboratory (NNL), NNL Preston Laboratory, Springfields, Salwick, Preston, PR4 0XJ, UK

* Corresponding Author. E-mail address: trgalvin1@sheffield.ac.uk

Abstract

Ti_3SiC_2 was deposited onto titanium substrates using electrophoretic deposition; a 4.3 wt.% suspension of Ti_3SiC_2 in water at pH 9 was used with 10 V field applied across the substrates. After 10 minutes of deposition, the coating surface density was 1.89±0.26 mg/cm^2. The thin coatings were then rapidly densified using a Renishaw AM250 3D printing laser to scan the surface. Cross sections of the substrate post sintering, showed the coating thickness to be 10–30 µm and densified with silicon loss constrained to the surface, although the overall coverage and adhesion varies. Preliminary Raman spectroscopy results suggest some MAX phase remains after sintering, but further characterisation is required to confirm.

Keywords: MAX phase, Ti_3SiC_2, Electrophoretic deposition (EPD), Coating, Laser sintering, Titanium

1. Introduction

$M_{n+1}AX_n$ phases are a family of ternary carbides and nitrides with a layered structure, which consist of a transition metal element, an A group element and carbon or nitrogen [1]. They have garnered interest in recent years due to their unusual combination of properties which include ceramic traits such as high stiffness, high temperature strength and resistance to creep, alongside properties more commonly found in metals such as good electrical and thermal conductivity, and they also have relatively high fracture toughness compared to other ceramics [2,3]. Due to their reasonable oxidation resistance and typically high decomposition temperature, MAX phases can be considered as a protective coating in many high temperature environments.Ti_3SiC_2 is arguably one of the most studied MAX phases; first discovered in the 1960's by Jeitschko and Nowotny [4], its unusual properties were largely unexplored until its 'rediscovery' by Barsoum and his research group at Drexel University [5], since which over 60 stable phases have been identified [6]. MAX phase 'A' layers can also be selectively etched, to produce thin films of MX layers known as MXenes, which are also of interest as a novel material [7].

There are several already established methods for depositing MAX phase coatings or synthesising thin films, including physical vapour deposition (PVD)[8], magnetron sputtering [9] and cathode arc deposition[10]. Other demonstrated techniques include cold-spraying [11][12][13], High velocity oxygen fuel (HVOF) spraying [14] and pulsed electrospark deposition [15]. Typically these methods require the coating or the substrate to be at an elevated temperature.

Electrophoretic deposition (EPD) is a frequently used coating technique, in which particles are suspended in a liquid medium. Due to the surface charge of these particles, measured by a quantity denoted ζ-potential, they move in suspension under the influence of an applied electric field between two electrodes. It is a useful coating process due to its relative ease, its application at room temperature and its ability to provide even coatings on complex geometries. Research into EPD of Ti_3SiC_2 and $Ti_3Si(Al)C_2$ has been carried out by Mishra et al. [16] and Liang et al.

[17] respectively. However, the green density of such coatings is typically quite low, and a sintering process is needed, which can be problematic due to delamination of the coating or excessive heating of the substrate. However, Wang et al. used a High Powered Diode Laser (HPDL) module affixed to a CNC controlled XY table to densify yttria stabilised zirconia and alumina coatings onto FeCrAl alloy substrates, minimising damage to the substrates [18]. De Riccardis et al. [19] have demonstrated a similar method for rapid densification of alumina-zirconia deposits using electron beam welding (EBW) equipment to scan the coated surface, resulting in densification, higher adhesion and thus demonstrating proof of concept the EPD powders can be densified on the surface of a given substrate.

Selective laser melting (SLM) is an additive manufacturing process whereby a high power laser is used to fuse particles (typically metal) in a powder bed under vacuum or inert gas. Under operation subsequent layers of powder are deposited on top and fused, building up a 3D part which is then removed from the bed of remaining un-densified powder. A related technique is Selective Laser Sintering (SLS), which does not melt the powder but rapidly sinters it (depending on the powder properties). Although these techniques are commonly associated with 3D printing, it was hypothesised that this could be a suitable method for densification of EPD ceramic layers of MAX phases. In this contribution, a SLM machine was utilised as a SLS machine (as MAX phases do not melt) within a vacuum chamber to scan a single layer over a green EPD MAX phase (Ti_3SiC_2) coating. The layers were then characterised using a combination of scanning electron microscopy (SEM) and Raman spectroscopy.

2. Materials and methods

Ti_3SiC_2 powder, containing about 10 vol.% of impurity TiC phase (Maxthal 312, Kanthal) was used as the feedstock in the experiments, due to its commercial availability. The pH adjustments during ζ-potential measurements were performed using dilute (0.1 M and 0.01 M) hydrochloric

acid and sodium hydroxide solutions. Titanium foil (1 mm thickness, Alfa-Aesar) was used as the substrate material to demonstrate proof of concept. Substrates were cut to 100 x 50mm sheets, and the surfaces wiped with isopropanol to remove any grease or fingerprints, and then with ethanoic acid to remove any oxides and further clean the surface. A final wash with distilled water removed any acid present.

2.1 Suspension preparation

The as-received Maxthal 312 was milled for 24 hours on a roller mill in isopropanol with ZrO_2 media to reduce the particle size and then dried at 80°C for a further 24 hours. Following the preparation from Liang et al. [17], suspensions were created using distilled water with a 4.3 wt.% addition of Ti_3SiC_2. The suspension was stirred with a glass rod for 2 minutes to break up any large agglomerates and to thoroughly 'wet' all the powder. The suspension was then ultrasonically agitated in a water bath for 5 minutes to break up any smaller agglomerates and to disperse the particles. Finally, the suspension was kept agitated using a magnetic stirrer and bar in between depositions to discourage flocculation (the agglomeration of fine particles formerly in suspension) and settling.

2.2 Deposition

Deposition was carried out using a power supply (Kikusui PAS500-0.6) connected to the titanium electrodes using a custom sample holder (modelled in Trimble SketchUp 2016 and 3D-printed in ABS plastic on custom built Prusa-Mendel type) to hold the substrates 15 mm apart in a 300 mL beaker (Fig.1). The voltage was kept at a constant while the current was monitored. After the allotted deposition time, the power supply was turned off and the receiving electrode was carefully removed and allowed to dry horizontally with the coated side facing up.

2.3 Sintering

Conventional sintering was undertaken at 1400°C under vacuum in a furnace (Elite TSF15-50/180-2416) with a hold time of 1 hour. Laser sintering was performed in a Renishaw AM250 SLM 3D printer using a modified pre-heat test programme under vacuum. The AM250 uses a pulsed laser to scan the surface. The energy deposition density was varied by adjusting the 1080 nm laser power and the beam focus (raising the focal point a set distance above the surface), thereby producing a matrix of squares.

2.4 Characterisation

The Ti_3SiC_2 was analysed in a Malvern Mastersizer 3000 to determine the distribution of particle sizes, using Mie scattering settings for non-spherical particles, and an obscuration level of 2.75% in water. Values for refractive index were estimated from work done by Ali et al. [20], and absorption was taken to be 1. ζ-potential measurements were taken at a range of pH values using a Malvern Zetasizer Nano to determine the maximum value (using the same parameters as particle size analysis). The coated plates were sectioned and set in Buehler Epoxicure 2 resin and left overnight to cure. The resin encased samples were polished using a Buehler Ecomet 250 with an Automet 250 head, using P260 and P600 diamond grinding discs (MetPrep Cameo Platinum Series) and then polished using 3 µm diamond suspension (MetPrep monocrystalline) on a cashmere cloth (MetPrep). SEM imaging and energy dispersive x-ray (EDX) analysis were performed on a Hitachi TM3030 (15kV) using the Bruker Quantax 70 software. Due to the uneven surface and inconsistent coverage, Raman was chosen as a characterisation tool as it requires a very small spot size. This was performed using a Renishaw InVia Raman microscope (625 nm 20 mW laser, 10 x 10s data accumulations).

3. Results

3.1 Particle size and zeta-potential

After milling, the median particle size of the Ti_3SiC_2 was 4.79 µm. As milling can lead to damage or contamination of the powder, and the size reduction was minimal, it is recommended that further work omits this step. Typically, particle sizes of 1-20 µm are appropriate for EPD [21], but smaller particle sizes increase the rate of deposition and lead to a denser coating. ζ-potential measurements are shown in Fig.2. For Ti_3SiC_2 in water, the isoelectric point (IEP, the value where the ζ-potential is 0 and the least optimum condition for a stable suspension) is at pH 5, while the maximum potential is between 9 and 9.5. This is the point where the particle repulsion is greatest, which means that flocculation and sedimentation are less likely. Suspensions were therefore adjusted to pH 9 before deposition.

3.2 Deposition

Deposition was carried out using 10 V, as higher voltages resulted in bubbles appearing in the coating due to electrolysis. Fig.3 displays the relationship between time and deposition mass density. After 10 minutes, the surface density was 1.89±0.26 mg/cm^2. During 10 minute depositions, the current fluctuated between 0.8 and 1 mA. Examining the green depositions under SEM (Fig.4) shows an even coverage of particles with a range of sizes, from 0.5 to 20 µm long.

3.3 Sintering

After conventional vacuum sintering, the coating delaminated into many small flakes. Although densification took place, the MAX phase did not adhere to the substrate, presumably as a result of differential thermal expansion between the Ti metal and the MAX phase.

The first test matrix varied laser power between 10 and 200 W in columns (10 x 21.11 W increments) and the focus of the beam between 0 and 14 mm in rows (8 x 2 mm increments). The 10 x 8 test squares were 5 mm squares, and the whole sintering process lasted around 40 seconds. Above 52W, the coating was ablated rather than densified and at low power and wide focus (5W, 10-14mm), the coating appears partially densified but delaminated. More encouraging, in between the results appeared successful. The substrate also began to curl and lift slightly with increasing laser power. Two subsequent matrices were performed on new substrates to try and better optimise the sintering conditions. These matrices featured reduced laser power ranges (5–50 W, 11.25W increments), focus ranges of 5–10 mm (1.67 mm increments) and 5–20 mm (5 mm increments) respectively, and a 5 x 4 array of larger 10 mm squares. Examining the plates under SEM, there were striking differences between the sintered and green areas of the plate. The path of the laser was clearly visible and there was localised fusing of the coating particles.

The effect of the laser focus parameter is shown in Fig.5 (31.1 W, 0–14mm focus). At narrow focus, the coating is ablated along the laser path, resulting in poor coverage and large globular regions of coating. As the beam becomes more diffuse, the effect is minimised and the coating coverage is improved with a reduction in tall surface agglomerates.

Fig. 6 shows a collection of cross sections of the coating. The thickness range is 10–30 µm and coverage and adhesion to the substrate varies. The section of 16.25 W and 10 mm, shows fairly uniform coverage, however the coating is cracked in places and shows some delamination from the surface of the Ti substrate. It is unclear if the delamination occurred during sintering or sectioning, but its adhesion here is poor. Whereas the 5 W, 5 mm sample shows periodic uneven coverage due to the narrow beam, but appears well adhered. There is also a prominent surface

phase which is cracked and poorly adhered to the coating. High power and wide focus (50 W, 10 mm) (Fig. 7) seems to offer good adhesion and slightly improved coverage, but gaps are still present and the surface phase is increased.

EDX spectra mapping of the cross section reveals that the surface phase is silicon-deficient (Fig. 8), and therefore is likely to be TiC_{1-x}, arising from the MAX phase decomposing through Si-loss [22]. There also appears to be very little in the way of diffusion into the substrate by the coating, likely due to the rapid nature of the bonding.

Fig. 9 shows Raman analysis of both the coating surface and the cross section. Characteristic peaks for Ti_3SiC_2 can be identified, along with a broad peak which is characteristic of sub-stoichiometric TiC [23]. This suggests that some of the coating remained crystalline during the sintering process.

4. Discussion

Low power and narrow focus results in the formation of periodic coverage bands seen in Fig. 8 (top left), increasing the power and broadening the focus results in the more consistent coating, but with poorer adhesion. Increasing the power results in wider bands that exhibit some cracking and have larger regions of the TiC_{1-x} surface phase. As shown in the cross-sections, there was significant delamination of the coating from the surface in some samples. The adhesion of the coating to substrate may be improved with a TiC interlayer, which could be deposited via EPD and conventionally or laser sintered before repeating the deposition with Ti_3SiC_2. Raman analysis shows characteristic peaks of Ti_3SiC_2, but a more comprehensive characterisation (such as TEM) is required to confirm what fraction of MAX phase remains after laser sintering.

The AM250 SLM machine has a spot size of approximately 70 μm at ‘zero’ focus parameter[24], which agrees with the width of the densified bands in the narrower focus images in Fig. 6. The hatching setting (distance between successive beam scans) was also approximately

70 µm and responsible for the spacing between the densified bands. A more easily parametrized laser setup would be beneficial in that accurate fluences could be determined. Taken as a whole, the results suggest that laser sintering of MAX phases on the surface of a metal substrate is feasible and points to a need for further work.

5. Conclusions

Thin coatings of green Ti_3SiC_2 were deposited onto titanium substrates electrophoretically for 10 minutes with 10 V, resulting in a surface green density of 1.89±0.26 mg/cm^2. After conventional attempts to densify and adhere the coating to the substrate were unsuccessful, a laser sintering approach was used to rapidly treat the surface. Varying the laser power and its focal length, resulted in a ~30 µm coating with either good coverage (low power and wide focus) or good adhesion (low power and narrow focus). 50 W and 10 mm focus showed improved coverage (with respect to the low power and narrow focus) while still remaining attached. Raman peaks were observed indicating the presence of Ti_3SiC_2 in the coating, but further examination is required to confirm the coating remained crystalline MAX phase, and to quantitatively determine its adhesion to the substrate.

Acknowledgements

This work was undertaken as part of a project funded from EPSRC and the NNL Internal R&D Programme Centre for Advanced Fuels under the Industrial CASE scheme (Grant no. 1614290). Some of the experiments were performed at the MIDAS facility at the University of Sheffield, which was established with financial support from the Department of Energy and Climate Change.

References

[1] M.W. Barsoum, The MAX Phases: A New Class of Solids; Thermodynamically Stable Nanolaminates, Prog Solid St Chem. 28 (2000) 201–281.

[2] M.W. Barsoum, MAX Phases: Properties of Machinable Ternary Carbides and Nitrides, in: Wiley-VCH, Wiley-, 2013. doi:10.1017/CBO9781107415324.004.

[3] M.W. Barsoum, T. El-raghy, C.J. Rawn, W.D. Porter, H. Wang, E. a Payzant, C.R. Hubbard, Thermal properties of Ti3 SiC2, J. Phys. Chem. Solids. 60 (1999) 429–439.

[4] W. Jeitschko, H. Nowotny, Die Kristallstruktur von Ti3SiC2—ein neuer Komplexcarbid-Typ, Monatshefte Für Chemie - Chem. Mon. 98 (1967) 329–337. doi:10.1007/BF00899949.

[5] M.W. Barsoum, T. El-Raghy, Synthesis and Characterization of a Remarkable Ceramic: Ti3SiC2, J. Am. Ceram. Soc. 79 (1996) 1953–1956.

[6] Z.M. Sun, Progress in research and development on MAX phases: a family of layered ternary compounds, Int. Mater. Rev. 56 (2011) 143–166. doi:10.1179/1743280410Y.0000000001.

[7] P. Eklund, J. Rosen, P.O.Å. Persson, Layered ternary Mn+1AXnphases and their 2D derivative MXene: An overview from a thin-film perspective, J. Phys. D. Appl. Phys. 50 (2017). doi:10.1088/1361-6463/aa57bc.

[8] P. Eklund, M. Beckers, U. Jansson, H. Högberg, L. Hultman, The Mn + 1AXnphases: Materials science and thin-film processing, Thin Solid Films. 518 (2010) 1851–1878. doi:10.1016/j.tsf.2009.07.184.

[9] C. Walter, D.P. Sigumonrong, T. El-Raghy, J.M. Schneider, Towards large area deposition of Cr2AlC on steel, Thin Solid Films. 515 (2006) 389–393. doi:10.1016/j.tsf.2005.12.219.

[10] M.C. Guenette, M.D. Tucker, M. Ionescu, M.M.M. Bilek, D.R. Mckenzie, Cathodic arc co-deposition of highly oriented hexagonal Ti and Ti 2 AlC MAX phase thin fi lms, Thin Solid Films. 519 (2010) 766–769. doi:10.1016/j.tsf.2010.09.007.

[11] S. Rech, A. Surpi, S. Vezzù, A. Patelli, A. Trentin, J. Glor, J. Frodelius, L. Hultman, P. Eklund, Cold-spray deposition of Ti 2 AlC coatings, Vacuum. 94 (2013) 69–73. doi:10.1016/j.vacuum.2013.01.023.

[12] H. Gutzmann, F. Gärtner, D. Höche, C. Blawert, T. Klassen, Cold spraying of Ti2AlC MAX-phase coatings, J. Therm. Spray Technol. 22 (2013) 406–412. doi:10.1007/s11666-012-9843-1.

[13] B.R. Maier, B.L. Garcia-Diaz, B. Hauch, L.C. Olson, R.L. Sindelar, K. Sridharan, Cold spray deposition of Ti2AlC coatings for improved nuclear fuel cladding, J. Nucl. Mater. 466 (2015) 1–6. doi:10.1016/j.jnucmat.2015.06.028.

[14] J. Frodelius, M. Sonestedt, S. Björklund, J.P. Palmquist, K. Stiller, H. Högberg, L. Hultman, Ti2AlC coatings deposited by High Velocity Oxy-Fuel spraying, Surf. Coatings Technol. 202 (2008) 5976–5981. doi:10.1016/j.surfcoat.2008.06.184.

[15] E.I. Zamulaeva, E.A. Levashov, T.A. Sviridova, N. V. Shvyndina, M.I. Petrzhik, Pulsed electrospark deposition of MAX phase Cr2AlC based coatings on titanium alloy, Surf. Coatings Technol. 235 (2013) 454–460. doi:10.1016/j.surfcoat.2013.08.002.

[16] M. Mishra, Y. Sakka, C. Hu, T.S. Suzuki, T. Uchikoshi, L. Besra, Electrophoretic deposition of Ti 3 SiC 2 and texture development in a strong magnetic field, J. Am. Ceram. Soc. 95 (2012) 2857–2862. doi:10.1111/j.1551-2916.2012.05296.x.

[17] Y. Liang, Z. Sun, J. Chen, X. Liu, Y. Zhou, Electrophoretic Deposition of Ti 3 Si(Al)C 2 from Aqueous Suspension, J. Am. Ceram. Soc. 1921 (2010) 1916–1921.

doi:10.1111/j.1551-2916.2010.03682.x.

[18] X. Wang, P. Xiao, M. Schmidt, L. Li, Laser processing of yttria stabilised zirconia/alumina coatings on Fecralloy substrates, Surf. Coatings Technol. 187 (2004) 370–376. doi:10.1016/j.surfcoat.2004.01.040.

[19] M.F. De Riccardis, D. Carbone, E. Piscopiello, M.V. Antisari, Electron beam treatments of electrophoretic ceramic coatings, Appl. Surf. Sci. 254 (2008) 1830–1836. doi:10.1016/j.apsusc.2007.07.164.

[20] M.S. Ali, A.K.M. a. Islam, M.M. Hossain, F. Parvin, Phase stability, elastic, electronic, thermal and optical properties of Ti3Al1−xSixC2 (0≤x≤1): First principle study, Phys. B Condens. Matter. 407 (2012) 4221–4228. doi:10.1016/j.physb.2012.07.007.

[21] L. Besra, M. Liu, A review on fundamentals and applications of electrophoretic deposition (EPD), Prog. Mater. Sci. 52 (2007) 1–61. doi:10.1016/j.pmatsci.2006.07.001.

[22] D.P. Riley, D.J.O. Connor, P. Dastoor, N. Brack, P.J. Pigram, Comparative analysis of Ti 3 SiC 2 and associated compounds using x-ray diffraction and x-ray photoelectron spectroscopy, 35 (2002) 1603–1611.

[23] B.H. Lohse, A. Calka, D. Wexler, Raman spectroscopy as a tool to study TiC formation during controlled ball milling, J. Appl. Phys. 97 (2005). doi:10.1063/1.1927282.

[24] “Renishaw’s laser melting” Am250 datasheet, Renishaw Plc. (2012).

Figure captions

Fig. 1 – Sample holder rendered in SketchUp (left) and experimental setup (right).

Fig. 2 – ζ potential measurements for Ti_3SiC_2 in water. Spread bars convey standard deviation.

Fig. 3 – Surface density of green coating against deposition time for Ti_3SiC_2 in pH 9 adjusted water.

Fig. 4 – SEM images showing coverage of green deposition at 10 V for 10 minutes. (Inset) Large MAX phase particle, ~20µm long.

Fig. 5 – SEM images of morphological effect of laser focus at 31.1W. Narrower focus results in poor coverage and ablation, while wider focus improves coverage.

Fig.6 - SEM images of laser-sintered coating cross sections at low and high magnification.

Fig.7 – SEM images of coating cross section with 50 W, 10 mm focus.

Fig.8– EDX spectra maps of resin mounted coating cross-section showing silicon-poor surface region. 5W laser power, 5mm focus.

Fig. 9 – Raman analysis of the surface and cross section of the coating, showing characteristic peaks for Ti_3SiC_2, and broad peak indicative of TiC_{1-x}.

Figures

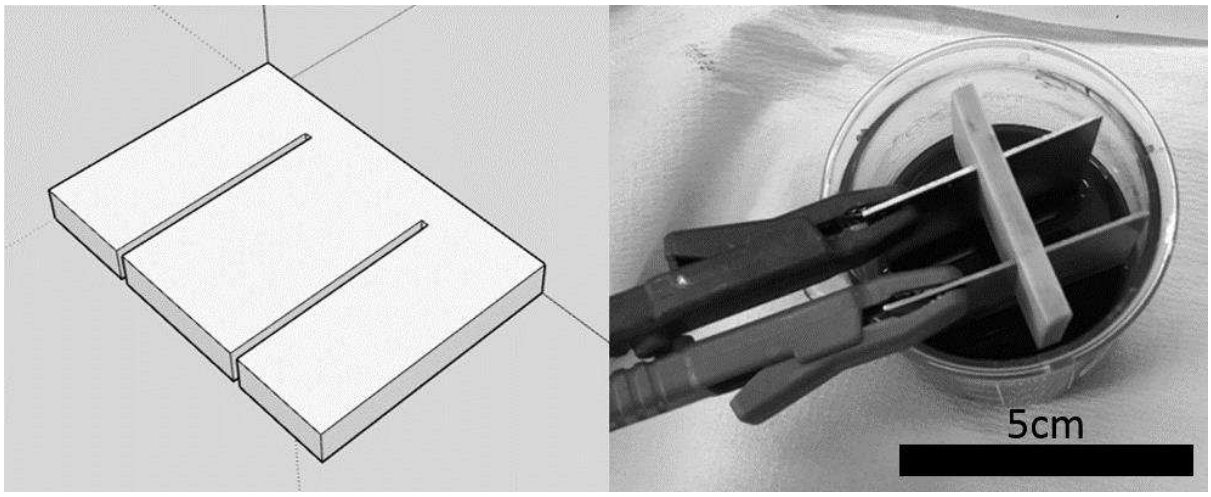

1

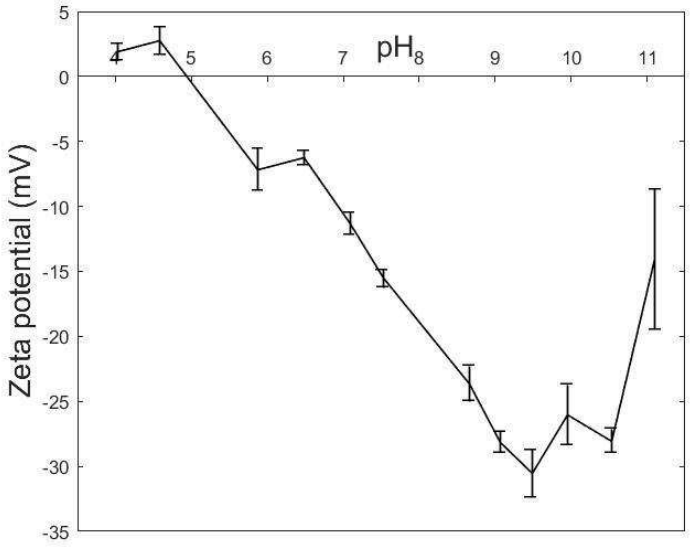

2

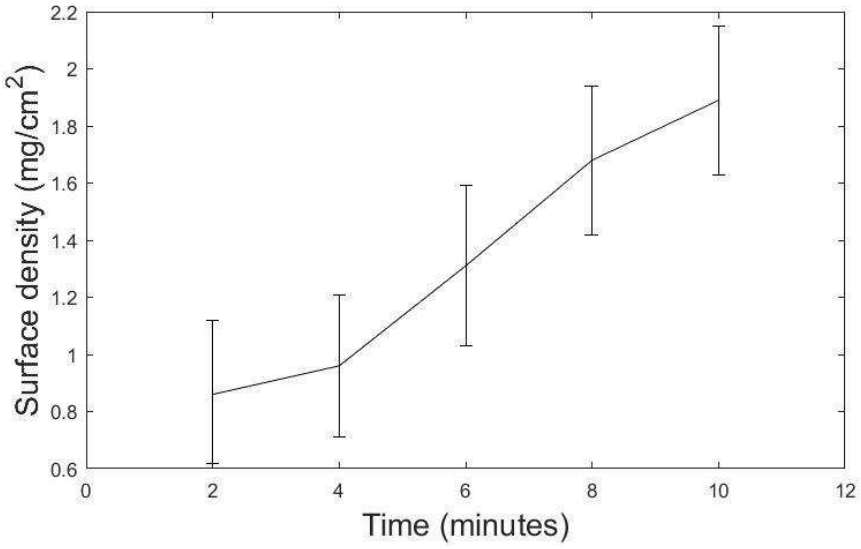
Surface density (mg/cm^2)
Time (minutes)
2.2
2
1.8
1.6
1.4
1.2
1
0.8
0.6
0
2
4
6
8
10
12

3

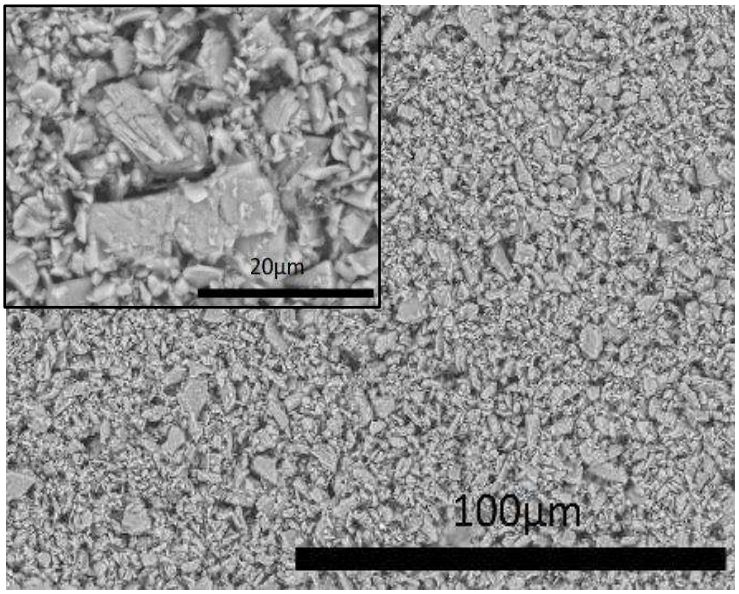
20µm
100µm

4

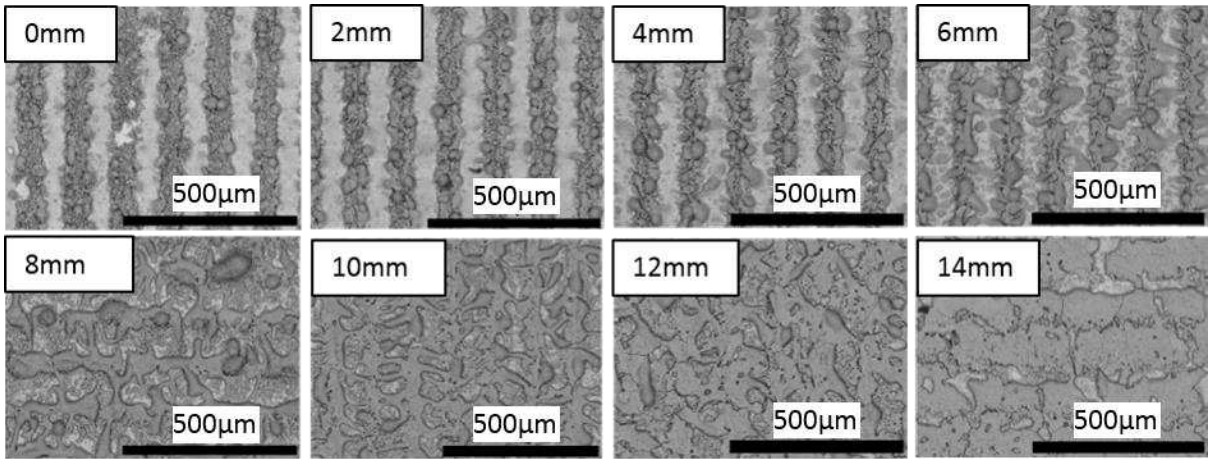
0mm
500µm
2mm
500µm
4mm
500µm
6mm
500µm
8mm
500µm
10mm
500µm
12mm
500µm
14mm
500µm

5

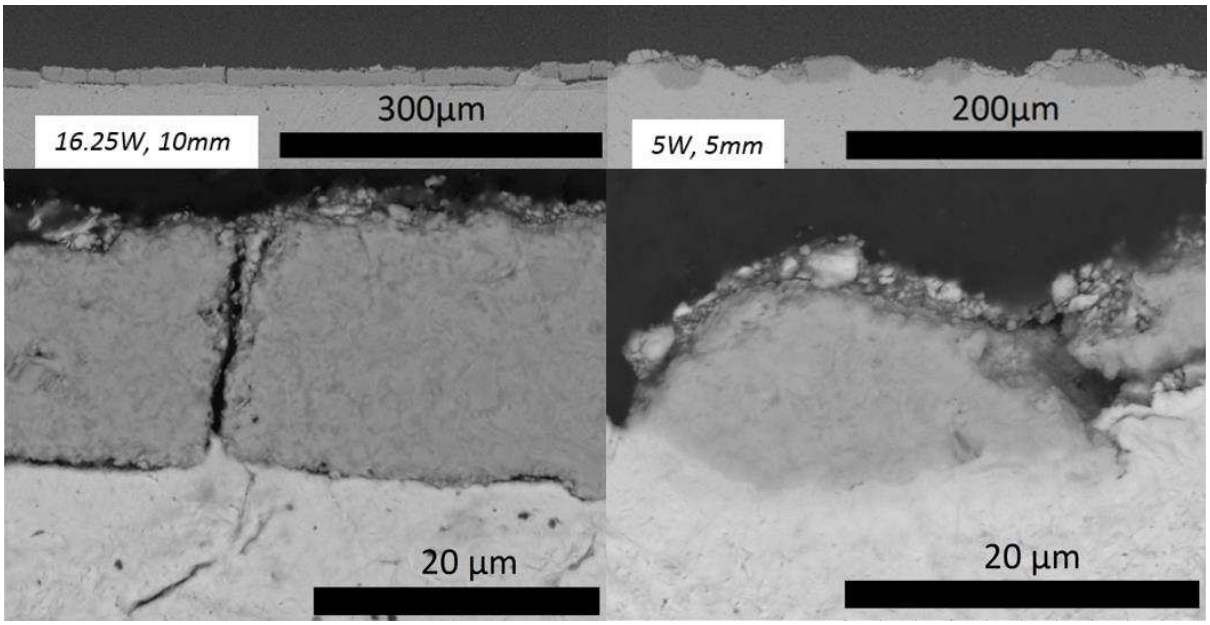
16.25W, 10mm
300µm
20 µm
5W, 5mm
200µm
20 µm

6

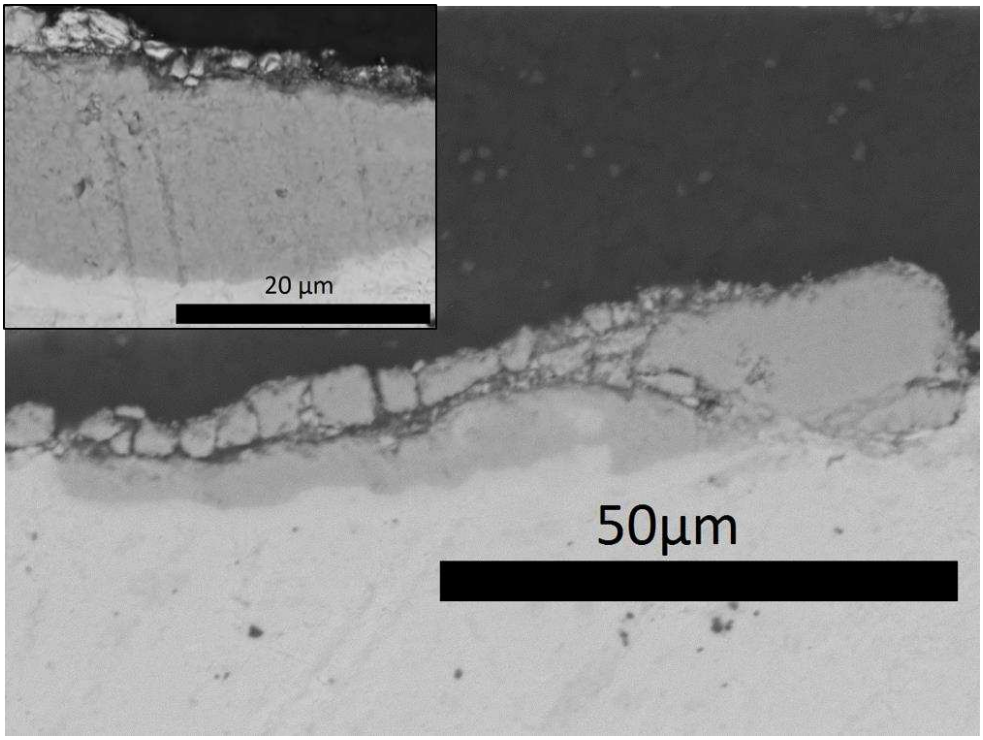

7

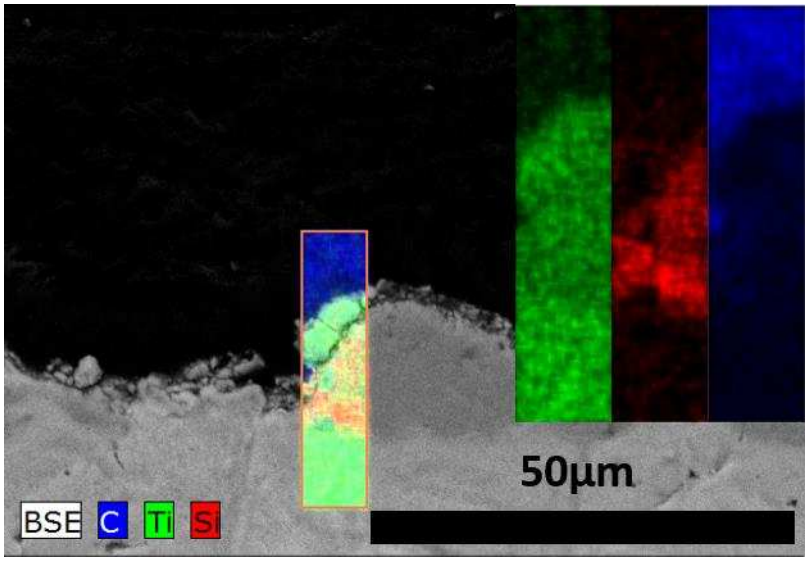

8 (colour figure)

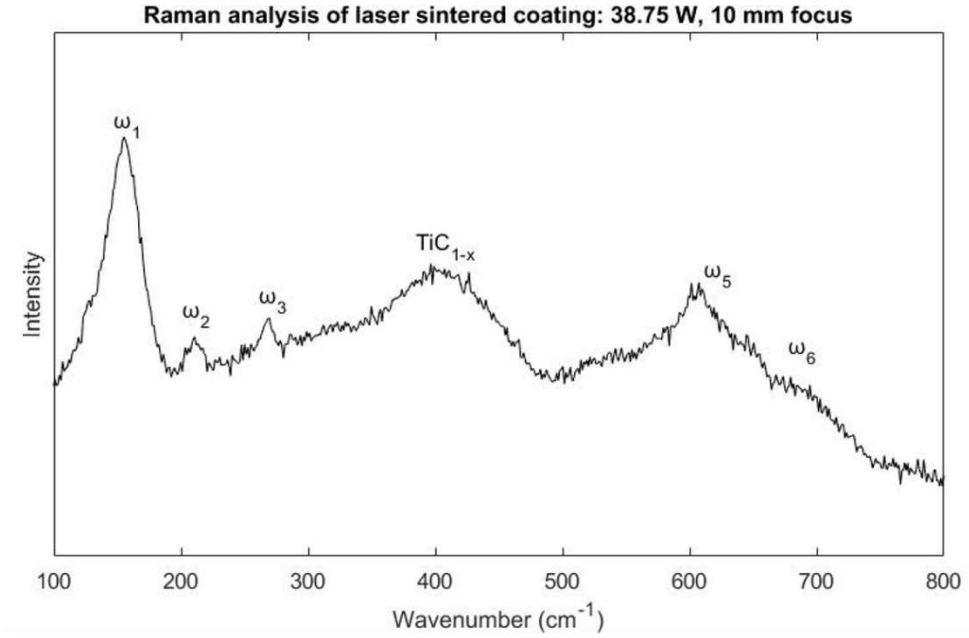
Raman analysis of laser sintered coating: 38.75 W, 10 mm focus
Intensity
ω1
ω2
ω3
TiC1-x
ω5
ω6
100
200
300
400
500
600
700
800
Wavenumber (cm-1)

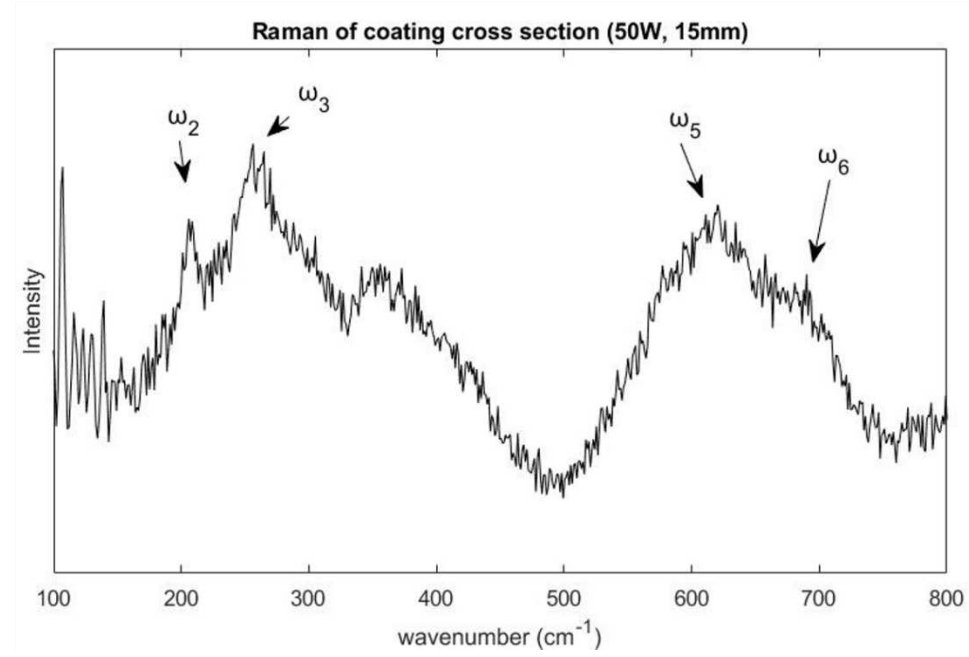
Raman of coating cross section (50W, 15mm)
Intensity
ω2
ω3
ω5
ω6
100
200
300
400
500
600
700
800
wavenumber (cm-1)

9